Laser and Particle Beams (2017), *35*, 543–550.
© Cambridge University Press, 2017 0263-0346/17
doi:10.1017/S0263034617000441

Twisted modes instability of electron–positron shell interacted with moving ion background

D. NOBAHAR, K. HAJISHARIFI,* AND H. MEHDIAN

Department of Physics and Institute for Plasma Research, Kharazmi University, 49 Dr. Mofatteh Avenue, Tehran 15614, Iran

(RECEIVED 16 April 2017; ACCEPTED 5 June 2017)

Abstract

In this paper, the instability of electrostatic twisted modes carrying orbital angular momentum in the moving electron–positron–ion plasma is investigated. In the kinetic theory approach, the general dispersion relation of twisted modes is derived by using Laguerre–Gaussian perturbed distribution function and electrostatic potential in the paraxial limit. Utilizing the obtained general dispersion relation for a specific case of electron–positron (e–p) shell with temperature anisotropy interacted with moving ion background, the effects of angular mode number, electrons and positrons temperature, and positron concentration on the group velocity and instability growth rate of twisted waves are illustrated, numerically. The results of the present investigation will greatly attribute to the understanding of e–p jet dynamic in astrophysical environments and laboratory experiments where the twisted modes can play a central role as a perturbed term.

Keywords: Electron–positron shell; Laguerre–Gaussian functions; Twisted plasma waves

1. INTRODUCTION

In recent years, the concept of twisted modes carrying orbital angular momentum (OAM) has been employed in the plasma systems. It is known that electromagnetic twisted wave not only has an intrinsic angular momentum (spin), but also has an OAM determined by the existence of helical phase front (Harris *et al.*, 1994; Leach *et al.*, 2002). At the first time, Mendonca *et al.* (2009) derived a paraxial equation of plasmon beams, as a superposition of twisted modes, to discuss its Gaussian and Laguerre–Gaussian (LG) beam solutions. Later, Leyser *et al.* (2009) have shown that such modes can be able to trap and transport the particles in the Earth's auroral zone and other space systems. In subsequent years, the other authors have used the hydrodynamic approach to depict the existence of OAM for phonons (Ayub *et al.*, 2011), electron waves in quantum plasmas (Khan *et al.*, 2013), dust-acoustic and ion-acoustic waves in dusty plasmas (Shukla, 2013), and coupled nonlinear electromagnetic waves in dense plasma systems (Shukla *et al.*, 2012). The kinetic theory has also been developed to investigate the Landau damping effect on the twisted electron modes (Mendonca, 2012), ion-acoustic plasma vortices (Khan *et al.*, 2014), twisted electron-acoustic waves (Rehman *et al.*, 2016), and so on. Apart from these, Ali *et al.* (2010), theoretically showed that in the presence of OAM of laser beam, the inverse Faraday phenomenon can be happened even for linearly polarized laser beam. Very recently, the kinetic study of electrostatic twisted wave instability in dusty plasma systems has been started by considering kappa distribution function for included components (Arshad *et al.*, 2017). In the present paper, the instability of the twisted modes excited in a drifting electron–positron (e–p) shell with Maxwellian distribution function on the moving ion background is investigated.

During the past few years, the study of electron–positron–ion (e–p–i) plasmas has attracted a great deal of attention (Berezhiani *et al.*, 1994; Saleem *et al.*, 2003; Shukla *et al.*, 2003; Amato & Arons, 2006; Baluku & Hellberg, 2011; Tinakiche & Annou, 2015; Mehdian *et al.*, 2016). Regarding the sufficient lifetime of positrons, it is believed that the combination of electrons, positrons, and ions to be an important ingredient of the early universe (Rees, 1983), and astrophysical medias such as pulsar magnetospheres (Goldreich & Julian, 1969), active galactic nuclei (Miller & Witter, 1987), interstellar clouds (Schlickeiser *et al.*, 2003), solar flares (Tandberg-Hansen & Emshie, 1988), accretion discs surrounding central black holes (Misner *et al.*, 1973), polar regions of neutron stars (Michel, 1991), and so on. As well as, in the some physical processes of laboratory environments

*Address correspondence and reprint requests to: K. Hajisharifi, Department of Physics and Institute for Plasma Research, Kharazmi University, 49 Dr. Mofatteh Avenue, Tehran 15614, Iran. E-mail: K.hajisharifi@gmail.com

https://doi.org/10.1017/S0263034617000441 Published online by Cambridge University Press

as in tokamak (Surko & Murphy, 1990) and in the systems including interaction of intense laser pulses with matter (Cowan *et al.*, 2000), the creation of e–p–i plasmas is not unexpected. One of the helpful methods to obtain some information about the physical properties of these systems is to investigate the stability conditions of them (Buneman, 1958; Haas *et al.*, 2000; Ali Shan *et al.*, 2008). It is known that the different drift velocities of species can supply the free energy source to drive the instability in the system (Verdon & Melrose, 2008). In this regard, a wide variety of studies have been done formerly by many researchers with considering the propagation of perturbed waves (Saleem & Khan, 2005; Ali Shan & Saleem, 2009; Nekrasov, 2009; Stockem *et al.*, 2015).

In this work, we consider an unmagnetized collisionless e–p–i plasma consisting of moving e–p shell and ion background. Coupling the Vlasov and Poisson equations and considering the LG perturbed distribution function and electrostatic potential in the paraxial limit, the generalized dispersion relation of perturbed twisted modes carrying OAM is obtained. Assuming Maxwellian velocity distribution function for the shell species in the plane normal to the perturbed wave propagation direction, the general dispersion relation is reduced to the simple form for the system under study. Solving the obtained dispersion relation numerically, the effects of angular mode number of twisted waves, positron concentration, and species temperature on the instability of the twisted modes in the system are investigated. The results show that, the angular mode number of twisted waves has a more important role on the growth rate of instability than longitudinal mode number.

This paper is organized as follows: the physical and theoretical models employed in our study are described in Section 2. Section 3 is devoted to the analysis of twisted modes instability based on the numerical solution of the obtained dispersion relation of perturbed twisted waves. Eventually, the conclusions and summary are presented in Section 4.

2. THEORETICAL MODEL AND EQUATIONS

Consider an unmagnetized collisionless e–p–i plasma system consisting of e–p shell drifting with the velocity v_0 through the moving ion background in the $\hat{z}$-direction. In the equilibrium state, the number density of the plasma components follows from the charge neutrality condition as $n_{e0} = n_{i0} + n_{p0}$, where the parameter of n_{e0}, n_{p0}, and n_{i0} indicate the equilibrium number density of electrons, positrons and ions, respectively. Moreover, the current density neutralization condition has been guaranteed by choosing the suitable drift velocities of plasma shell and background ions. It is assumed that the electrostatic twisted mode with slowly varying amplitude, mentioned in (Mendonca *et al.*, 2009), perturbs the initial equilibrium of the system. Neglecting the background ions perturbation and employing the kinetic theory to study of the system, the distribution function for α-th shell species can be written linearly as sum of the unperturbed and perturbed distribution function as $f_\alpha = f_{\alpha 0} + f_{\alpha 1}$. For this system the linearized Vlasov equation can be written as

$$\frac{\partial}{\partial t} f_{\alpha 1} + \boldsymbol{v}.\boldsymbol{\nabla} f_{\alpha 1} + \frac{q_\alpha}{m_\alpha}\boldsymbol{E}.\frac{\partial}{\partial \boldsymbol{v}} f_{\alpha 1} = 0, \tag{1}$$

in which $\boldsymbol{E} = -\boldsymbol{\nabla}\phi$ is the perturbed electric field, where ϕ is the perturbed LG electric potential satisfying the linearized Poisson equation

$$\nabla^2\phi = -4\pi \sum_\alpha q_\alpha \int f_{\alpha 1}(\boldsymbol{r}, \boldsymbol{v}, t) d\boldsymbol{v}. \tag{2}$$

By using the LG equation $(\nabla_\perp^2 + 2ik_z(\partial/\partial z))\phi(\boldsymbol{r}, t) = 0$ for the electrostatic twisted wave propagation along the $\hat{z}$-direction with slowly varying amplitude, Eq. (2) can be reduced to

$$k^2\phi(\boldsymbol{r}, t) = 4\pi \sum_\alpha q_\alpha \int f_{\alpha 1}(\boldsymbol{r}, \boldsymbol{v}, t) d\boldsymbol{v}, \tag{3}$$

in which use is made of Laplacian operator $\nabla^2 = \nabla_\perp^2 - k^2 + 2ik(\partial/\partial z)$. From Appendix (A), the electrostatic potential in the paraxial limit is given by

$$\phi(\boldsymbol{r}, t) = \sum_{jl} \tilde{\phi}_{jl} F_{jl}(r, z) \exp(il\theta + ik_z z - i\omega t). \tag{4}$$

Replacing Eq. (4) in Eq. (3), the perturbed distribution function in terms of LG functions can be expressed as follows:

$$f_{\alpha 1}(\boldsymbol{r}, \boldsymbol{v}, t) = \sum_{jl} \tilde{f}_{jl}(\boldsymbol{v}) F_{jl}(r, z) \exp(il\theta + ik_z z - i\omega t). \tag{5}$$

Substituting Eqs. (4) and (5) into Eq. (1) and integrating it over radial component, the perturbed distribution function can be obtained as

$$\tilde{f}_{jl}(\boldsymbol{v}) = \sum_\alpha \frac{q_\alpha}{m_\alpha} \frac{\tilde{\phi}_{jl}}{(a + ib)} \left(\boldsymbol{q}_{eff}.\frac{\partial f_{\alpha 0}}{\partial \boldsymbol{v}}\right), \tag{6}$$

where

$$\boldsymbol{q}_{\text{eff}} = -iq_r\hat{\boldsymbol{e}}_r + lq_\theta\hat{\boldsymbol{e}}_\theta + (k - iq_z)\hat{\boldsymbol{e}}_z. \tag{7}$$

In Eq. (6), the parameters a and b are defined as $a = \omega - kv_z - lq_\theta v_\theta$ and $b = q_r v_r + q_z v_z$, where $q_r = \int_0^\infty rF_{jl}(\partial F_{jl}/\partial r)\mathrm{d}r$, $q_\theta = \int_0^\infty F_{jl}^2 \mathrm{d}r$, and $q_z = \int_0^\infty rF_{jl}\frac{\partial F_{jl}}{\partial z}\mathrm{d}r$. Substituting Eqs. (4–6) into Eq. (3), the general dispersion relation becomes

$$D(k, \omega) = 1 - \sum_\alpha \frac{\omega_{p\alpha}^2}{k^2} \int \frac{\boldsymbol{q}_{\text{eff}}.(\partial f_{\alpha 0}/\partial \boldsymbol{v})}{\omega - \boldsymbol{q}_{\text{eff}}.\boldsymbol{v}} d\boldsymbol{v} = 0. \tag{8}$$

The above equation is formally similar to the dispersion relation of the plane waves, except that the Landau resonance frequency

https://doi.org/10.1017/S0263034617000441 Published online by Cambridge University Press

in the presence of helical electric field occurs at

$$\omega = kv_z + lq_\theta v_\theta \pm i(q_r v_r + q_z v_z). \tag{9}$$

In order to investigate the explicit effect of OAM on the obtained dispersion relation, we consider the approximation limit $|q_r|, |q_z| << |lq_\theta|$. In this limit, the modified resonance condition can be written as $\omega = kv_z + lq_\theta v_\theta$, in which the additional factor $lq_\theta v_\theta$ indicates the effect of OAM of the twisted wave on the resonance frequency. Now, Eq. (8) can be reduced to

$$D(k, \omega) = 1 - \sum_\alpha \frac{\omega_{p\alpha}^2}{k^2} \int \frac{lq_\theta(\partial f_{\alpha 0}/\partial v_\theta) + k(\partial f_{\alpha 0}/\partial v_z)}{\omega - kv_z - lq_\theta v_\theta} d\boldsymbol{v} = 0. \tag{10}$$

Or its expansion

$$D(k, \omega) = 1 - \sum_\alpha \frac{\omega_{p\alpha}^2}{k^2} \left\{ \int \frac{(\partial f_{\alpha 0}/\partial v_z)}{(\omega - lq_\theta v_\theta/k) - v_z} \mathrm{d}\boldsymbol{v} + \int \frac{(\partial f_{\alpha 0}/\partial v_\theta)}{(\omega - kv_z/lq_\theta) - v_\theta} \mathrm{d}\boldsymbol{v} \right\}. \tag{11}$$

the additional degree of freedom of temperature anisotropy, the equilibrium distribution function of shell species is considered as

$$f_{\alpha 0}(v_\perp, v_z) = f_{\alpha 0}(v_r, v_\theta)\delta(v_z - v_{0\alpha}). \tag{13}$$

This temperature anisotropic distribution function represents streaming shell with the constant velocity $v_z = v_{0\alpha}$ along the $\hat{z}$-direction ($T_\parallel = 0$), and with thermal distribution function in the plane normal to $\hat{z}$, ($T_\perp \neq 0$). The perpendicular distribution function of the shell components, $f_{\alpha 0}(v_\perp)$, are given by Maxwellian distribution function

$$f_{\alpha 0}(v_r, v_\theta) = \frac{m_\alpha}{2\pi k_B T_\alpha} \exp\left[-\frac{m_\alpha v_\perp^2}{2k_B T_\alpha} \right]. \tag{14}$$

Substituting Eqs. (14) and (13) into Eq. (12), the dispersion relation becomes

$$D(k, \omega) = 1 + \sum_{\alpha=e,P} \frac{\omega_{p\alpha}^2}{k^2} \left\{ \frac{k^2}{\omega^2} \left(1 + 2v_{0\alpha}\frac{k}{\omega} + 3v_{0\alpha}^2 \frac{k^2}{\omega^2} \right) + \frac{(lq_\theta)^2}{(\omega - kv_{0\alpha})^2} \left(1 + \frac{3V_{T\alpha}^2 (lq_\theta)^2}{4(\omega - kv_{0\alpha})^2} \right) + \frac{2i\sqrt{\pi}}{V_{T\alpha}^3} \left(1 + \frac{k^2}{(lq_\theta)^2} \right) \left(\frac{\omega - kv_{0\alpha}}{lq_\theta} \right) \exp\left[-\frac{1}{V_{T\alpha}^2} \left(\frac{\omega - kv_{0\alpha}}{lq_\theta} \right)^2 \right] \right\}, \tag{15}$$

Using the Plemelj formula, the above relation becomes

$$D(k, \omega) = 1 + \sum_\alpha \frac{\omega_{p\alpha}^2}{k^2} \left\{ \mathcal{P} \int \left[\frac{(\partial f_{\alpha 0}/\partial v_z)}{v_z - u_z} + \frac{(\partial f_{\alpha 0}/\partial v_\theta)}{v_\theta - u_\theta} \right] \mathrm{d}\boldsymbol{v} + i\pi \int \left[\left(\frac{\partial f_{\alpha 0}}{\partial v_z} \right) \delta(v_z - u_z) + \left(\frac{\partial f_{\alpha 0}}{\partial v_\theta} \right) \delta(v_\theta - u_\theta) \right] \mathrm{d}\boldsymbol{v} \right\}, \tag{12}$$

where $\mathcal{P}$ is the principle value of integral, $v_z = (\omega - lq_\theta v_\theta)/k$, and $v_\theta = (\omega - lq_\theta v_z)/k$. To analyze the two-stream like instability of kinetic-model plasma equilibrium with in which $V_{T\alpha} = \sqrt{(2k_B T_\alpha/m_\alpha)}$ is the thermal speed of α-th species. This equation is formally different from the dispersion relation of the plane wave in the same configuration, where the additional contribution arises from the azimuthal term of the twisted modes. It should be noted that, in the limit of $l \to 0$, Eq. (15) reduces to the familiar form of the plane wave dispersion relation. Using the normalized parameters defined as

$$\Omega = \frac{\omega}{\omega_{pe}}, \quad K_z = \frac{kv_{0e}}{\omega_{pe}}, \quad K_\theta = \frac{lq_\theta v_{0e}}{\omega_{pe}}, \quad N_P = \frac{\omega_{pP}^2}{\omega_{pe}^2},$$
$$\beta = \frac{v_{0P}}{v_{oe}}, \quad \alpha_1 = \frac{V_{Te}}{v_{0e}}, \quad \alpha_2 = \frac{V_{TP}}{v_{0P}},$$

the obtained dispersion relation (15) can be written in the normalized form as

$$1 + \frac{1}{\Omega^4}\left[(1 + N_P)\Omega^2 + 2K_z(1 + N_P\beta)\Omega + 3K_z^2(1 + N_P\beta^2) \right] + \frac{K_\theta^2}{4K_z^2} \times \left[3K_\theta^2 \left(\frac{\alpha_1^2}{(K_z - \Omega)^4} + \frac{N_P\alpha_2^2\beta^2}{(\Omega - K_z\beta)^4} \right) + 4\left(\frac{1}{(K_z - \Omega)^2} + \frac{N_P}{(\Omega - \beta K_z)^2} \right) \right] + i\frac{2\sqrt{\pi}(K_z^2 + K_\theta^2)}{K_z^2 K_\theta^2} \times \left[\frac{(\Omega - K_z)}{\alpha_1^3} \exp\left(\frac{-(\Omega - K_z)^2}{K_\theta^2 \alpha_1^2} \right) + \frac{N_P(\Omega - \beta K_z)}{\beta^2 \alpha_2^2} \exp\left(-\frac{(\Omega - \beta K_z)^2}{\beta^2 \alpha_2^2 K_\theta^2} \right) \right] = 0. \tag{16}$$

https://doi.org/10.1017/S0263034617000441 Published online by Cambridge University Press

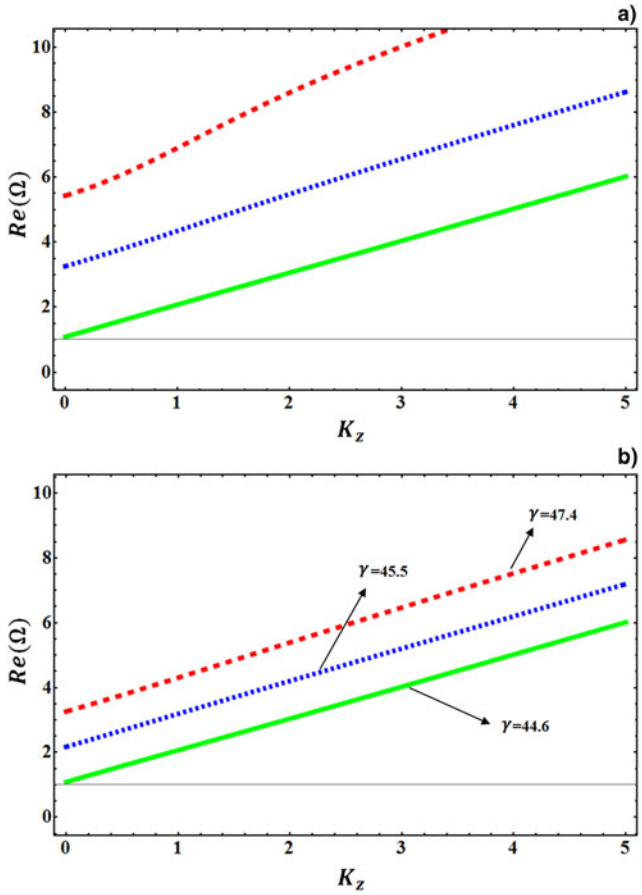


Fig. 1. The variation of normalized real frequency [$\mathrm{Re}(\Omega) = (\omega/\omega_{pe})$] of twisted waves as a function of normalized longitudinal wave number ($K_z = kv_{0e}/\omega_{pe}$) for $\beta = 1$, $N_P = 0.5$ and (a) $K_\theta = 2$, $\alpha_1 = \alpha_2 = 1/2$ (solid green curve), $\alpha_1 = \alpha_2 = 3/2$ (dotted blue curve), $\alpha_1 = \alpha_2 = 5/2$ (dashed red curve), and (b) $\alpha_1 = \alpha_2 = 1$, $K_\theta = 1$ (solid green curve), $K_\theta = 2$ (dotted blue curve), and $K_\theta = 3$ (dashed red curve). γ is the slope of curves.

As can be seen, this relation is difficult to be solved analytically, so in the next section the numerical method will be employed to analyze the instability growth rate of the twisted modes.

3. NUMERICAL RESULTS AND DISCUSSION

In this section, the numerical method has been employed to solve the normalized dispersion relation (16) by considering the charge and current neutralization conditions as $n_{e0} = n_{P0} + n_{i0}$, and $n_{e0}v_{e0} = n_{P0}v_{P0} + n_{i0}v_{i0}$, respectively. Let us assume the unperturbed velocity of the plasma shell be $v_{e0} = v_{P0} = v_0$.

Figure 1 represents the variation of normalized real frequency [Re(Ω)] of twisted waves as a function of normalized wave number K_z for the chosen system parameter values $\beta = 1$, $N_P = 0.5$, $K_\theta = 2$, and $\alpha_1 = \alpha_2 = 1/2$, $3/2$, $5/2$ in Figure 1(a), and $\beta = 1$, $N_P = 0.5$, $\alpha_1 = \alpha_2 = 1$, and $K_\theta = 1$, 2, 3 in Figure 1(b). As seen in Figure 1(a), for fixed value of azimuthal wave number, increasing the ratio of $\alpha(= \alpha_1 = \alpha_2)$ increases the slope of curves and so causes to increment of the group velocity of twisted waves. As well as, Figure 1(b) shows that for fixed value of normalized parameter α, the twisted waves group velocity increases very slowly (not so considerable) by the azimuthal wave number.

The effect of increasing of the parameter α on the variation of [$Re(\Omega)$] for twisted waves is illustrated three dimensionally in Figure 2 for chosen quantities $\beta = 1$, $N_P = 0.5$, $\alpha_1 = \alpha_2 = 1/2$ in Figure 2(a), and $\beta = 1$, $N_P = 0.5$, $\alpha_1 = \alpha_2 = 3/2$ in Figure 2(b). We see that in Figure 2(a) and 2(b), increasing the longitudinal and azimuthal wave number increases the real part of frequency (phase velocity of wave). By comparing these two figures, it can be concluded that the phase and group velocities are enhanced by increasing the parameter α.

The effect of angular wave number on the instability of the excited twisted waves has been depicted in Figure 3. This figure exhibits the variation of normalized growth rate [$Im(\Omega)$] versus normalized longitudinal wave number (K_z) for several values of K_θ ranging from $K_\theta = 1$ to $K_\theta = 6$ with keeping constant the other parameter values (α, β, and N_p). As seen clearly, for each given K_θ and any arbitrary K_z the growth rate curves show a non-zero value and a little bump around the specified wave number K_0, called the critical wave number.

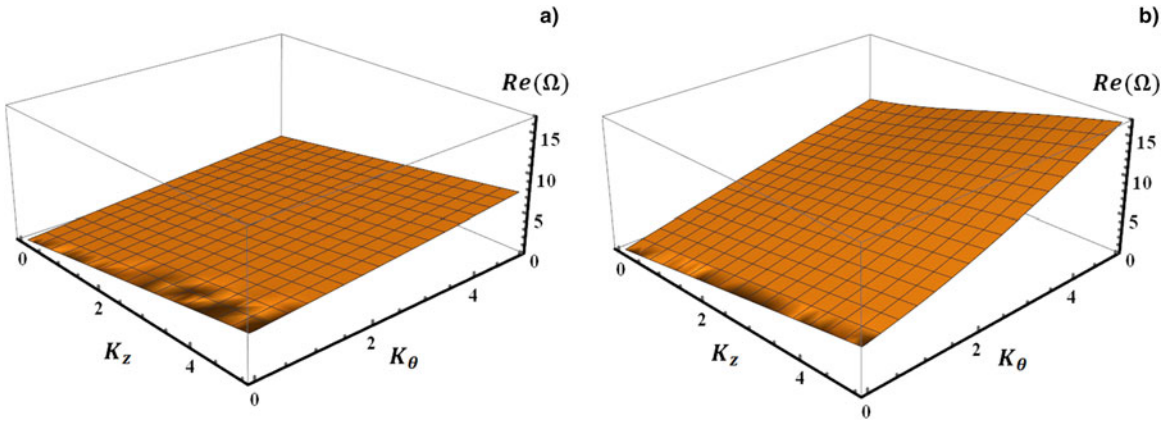


Fig. 2. The 3D view of normalized real frequency of twisted waves in terms of K_z and K_θ for (a) $\alpha_1 = \alpha_2 = 1/2$ and (b) $\alpha_1 = \alpha_2 = 3/2$.

https://doi.org/10.1017/S0263034617000441 Published online by Cambridge University Press

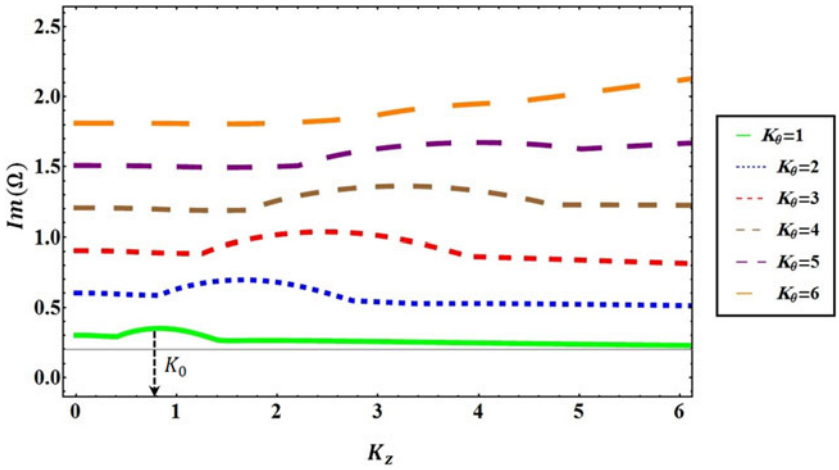


Fig. 3. The normalized growth rate as a function of normalized longitudinal wave number for fixed values of $\alpha = 1/2, \beta = 1, N_P = 0.5$ and different value of K_θ.

The critical wave number as well as the band width of the bumps increase with increasing K_θ. Moreover, for fixed value of longitudinal wave number, the growth rate dramatically increases with azimuthal wave number.

Figure 4 shows the variation of normalized growth rate [$Im(\Omega)$] versus normalized longitudinal wave number (K_z) for different values of α ranging from $\alpha = 0.2$ to $\alpha = 1.4$ with keeping constant quantities of K_θ, β, and N_p. In Figure 4, for a specified value of K_z, the growth rate increases by increasing α. On the other hand, for $\alpha<1$ the width and height of the bump of the growth rate curves increase by enhancing the values of α, and then the growth rate eventually saturates after the turning point. While for $\alpha>1$ in which the thermal speed of electrons and positrons is larger than the shell velocity, the instability of twisted waves enhances and, consequently, the system will be highly unstable on the electron time scale. It seems that the reason of this behavior arises from the enhancement of the free energy originating from increment of the thermal motion of shell components.

The dependence of the growth rate of twisted wave in our system on the magnitude of N_p is demonstrated in Figure 5. In this figure, the normalized growth rate as a function of normalized longitudinal and azimuthal wave number is shown three dimensionally for $N_p = 0.1$ and 0.5 with corresponding contour plot of them. Comparing Figure 5(a) and 5(b), it is deduced that when the concentration of positron in the system is diminished the growth rate of the twisted mode is enhanced. In addition to, the contour plot of these figures [Figure 5(c) and 5(d)] show that for a fixed value of K_z the variations of growth rate are more than those for a fixed value of K_θ. In other words, azimuthal wave number has a more important role on the growth rate than the longitudinal wave number.

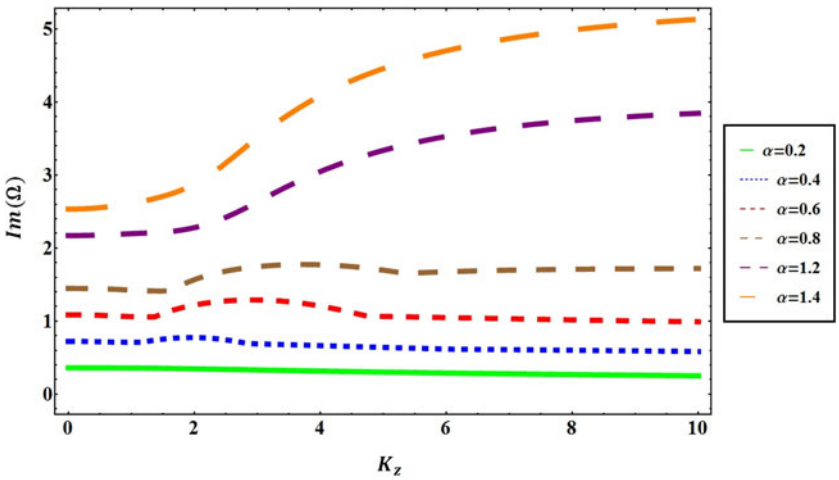


Fig. 4. The normalized growth rate as a function of normalized longitudinal wave number for fixed values of $K_\theta = 3, \beta = 1, N_P = 0.5$ and different value of α.

https://doi.org/10.1017/S0263034617000441 Published online by Cambridge University Press

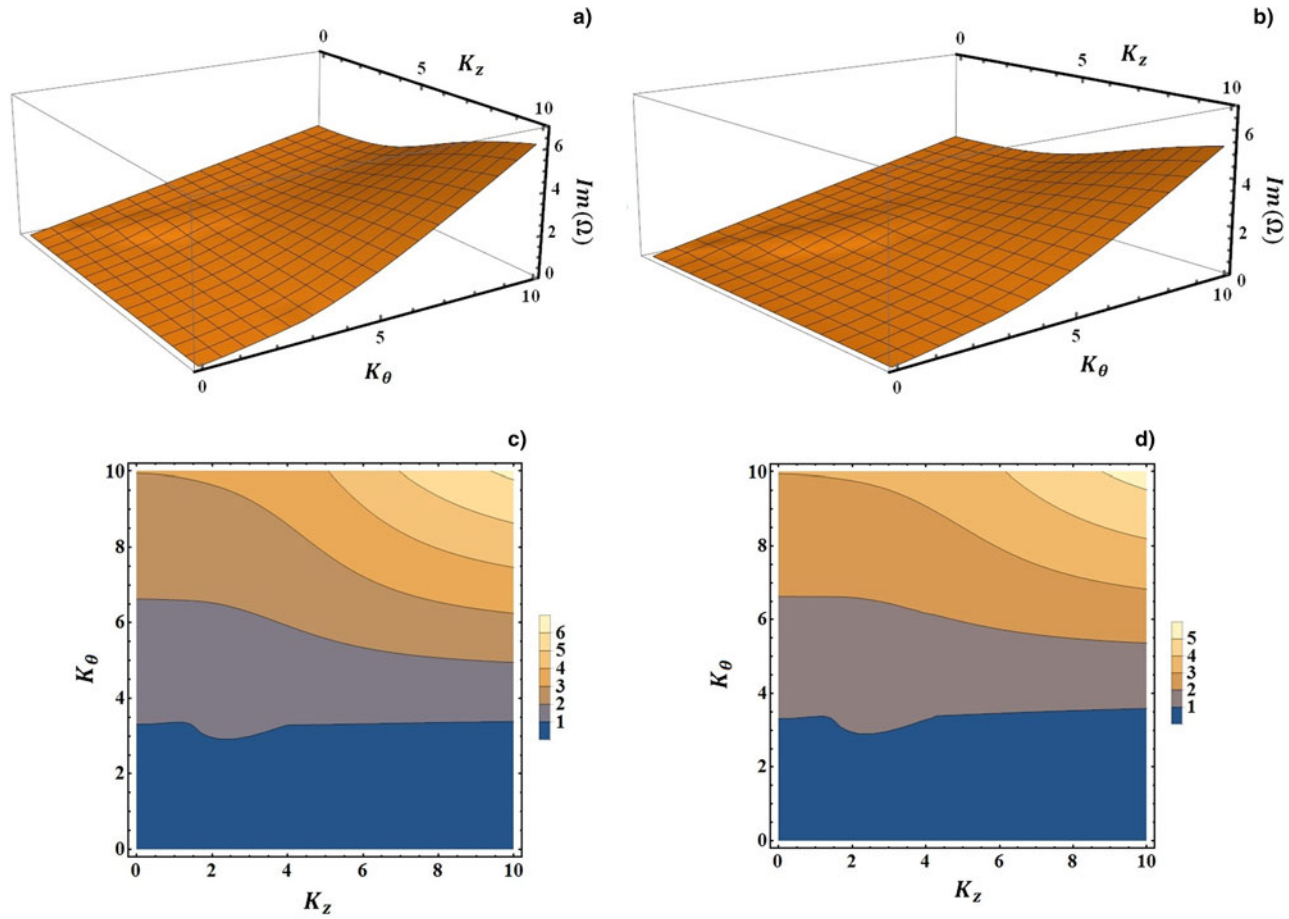


Fig. 5. The 3D view of normalized growth rate as a function of normalized longitudinal and azimuthal wave number for (a) $N_p = 0.1$, $\alpha = 1/2$, $\beta = 1$, and (b) $N_P = 0.5$, $\alpha = 1/2$, $\beta = 1$ with a corresponding contour plots of them.

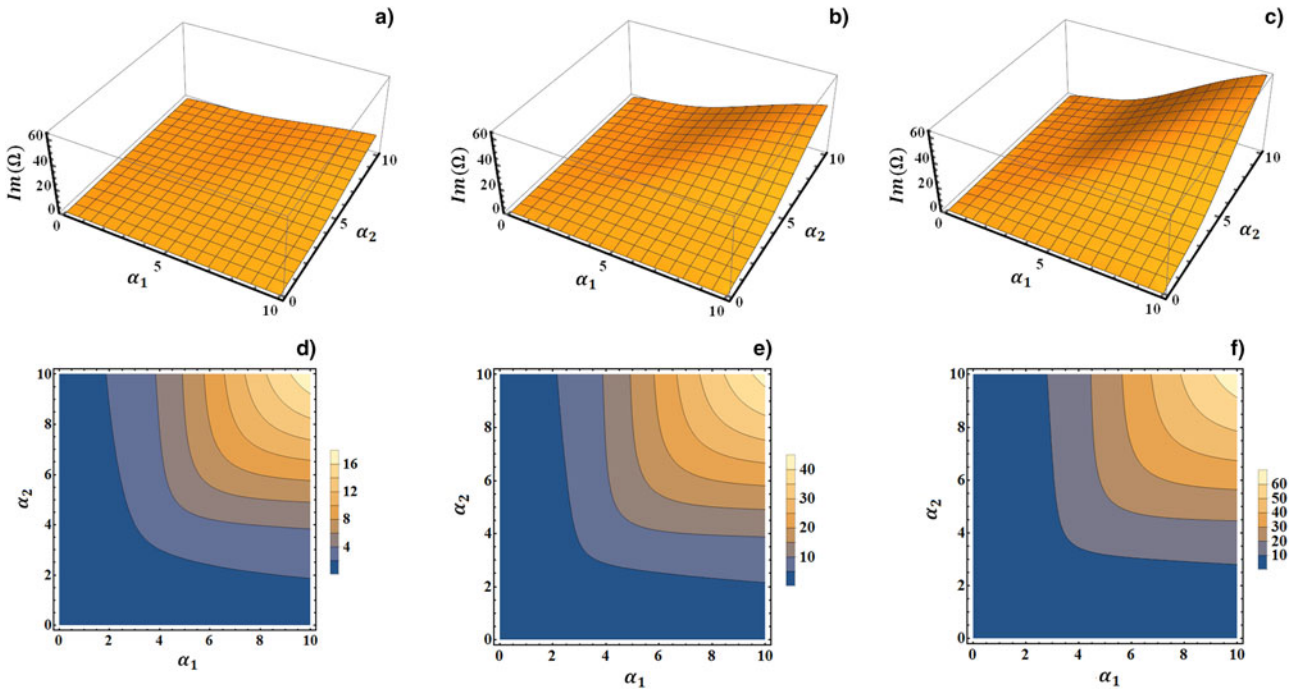


Fig. 6. The 3D view of normalized growth rate as a function of $\alpha_1 = V_{Te}/v_{0e}$ and $\alpha_2 = V_{TP}/v_{0P}$ with a corresponding contour plots for (a, d) $K_\theta = 1$, $K_z = 1$, $\beta = 1$, $N_P = 0.5$, (b, e) $K_\theta = 2$, $K_z = 1$, $\beta = 1$, $N_P = 0.5$, (c, f) $K_\theta = 3$, $K_z = 1$, $\beta = 1$, $N_P = 0.5$.

https://doi.org/10.1017/S0263034617000441 Published online by Cambridge University Press

Finally, we close this investigation by plotting the three-dimensional (3D) view of normalized growth rate as a function of α_1 and α_2 to show the role of $K_\theta = 1, 2, 3$ in the variation of growth rate for $K_z = 1$, $N_P = 0.5$, and $\beta = 1$. From Figure 6 it is concluded that, by increasing the value of K_θ the amount of growth rate increases. Furthermore, for the fixed values of K_z and K_θ the growth rate increases with α_1 and α_2. Also, Figure 6(d), 6(e), and 6(f) which are the corresponding contour plots of Figure 6(a), 6(b), and 6(c), respectively, display that only for a small values (arbitrary value) of α_1 and arbitrary value (small values) of α_2 the amount of growth rate are approximately constant. Of course this interval of constant growth rate increases by increasing the value of K_θ.

4. SUMMARY AND CONCLUSION

In this paper, the kinetic approach has been used to study the instability of the twisted wave carrying OAM in an unmagnetized collisionless plasma system containing of e–p shell drifting through the moving ion background. Considering the electrostatic potential in the paraxial limit and employing the LG perturbed distribution function, the Vlasove–Poisson equation has been solved to derive the dispersion relation of perturbed twisted waves in the given temperature anisotropic system. Based on the numerical analysis, the behavior of instability growth rate of twisted modes has been investigated in detail. It has been found that the instability of the electrostatic twisted wave increases by angular mode number, and this increment is more considerable for high values of shell temperature. Moreover, the growth rate diminishes with enhancement of the positron concentration in the system. In addition to, the results show that the impact of azimuthal wave number on the increasing of the growth rate is larger than longitudinal wave number. Our results can be applied to experimental processes such as in inertial confinement fusion where the interaction of high-power laser with matter produces an e–p shells (Chen *et al.*, 2013), and to astrophysical systems like as gamma-ray burst in the presence of e–p winds (Geng *et al.*, 2016).

REFERENCES

Ali, S., Davies, J.R. & Mendonca, J.T. (2010). Inverse faraday effect with linearly polarized laser pulses. *Phys. Rev. Lett.* **105**, 035001.

Ali Shan, S. & Saleem, H. (2009). Kinetic effects on streaming instabilities in electron–positron-ion plasmas. *Phys. Plasmas* **16**, 022111.

Ali Shan, S., Saleem, H. & Sajid, M. (2008). Streaming instabilities in multicomponent interstellar clouds. *Phys. Plasmas* **15**, 072904.

Amato, E. & Arons, J. (2006). Heating and nonthermal particle acceleration in relativistic, transverse magnetosonic shock waves in proton–electron–positron plasmas. *Astrophys. J.* **653**, 325–338.

Arshad, K., Lazar, M., Mahmood, Sh., Ur-Rehman, A. & Poedts, S. (2017). Kinetic study of electrostatic twisted waves instability in nonthermal dusty plasmas. *Plasma Phys.* **24**, 033701.

Ayub, M.K., Ali, S. & Mendonca, J.T. (2011). Phonons with orbital angular momentum. *Phys. Plasmas* **18**, 102117.

Baluku, T.K. & Hellberg, M.A. (2011). Ion acoustic solitary waves in an electron–positron–ion plasma with non-thermal electrons. *Plasma Phys. Control. Fusion* **53**, 095007.

Berezhiani, V.I., El-Ashry, M.Y. & Mofiz, U.A. (1994). Theory of strong-electromagnetic-wave propagation in an electron–positron–ion plasma. *Phys. Rev. E* **50**, 448.

Buneman, O. (1958). Instability, turbulence, and conductivity in current-carrying plasma. *Phys. Rev. Lett.* **1**, 119.

Chen, H., Nakai, M., Sentoku, Y., Arikawa, Y., Azechi, H., Fujioka, S., Keane, C., Kojima, S., Goldstein, W., Maddox, B.R., Miyanaga, N., Morita, T., Nagai, T., Nishimura, H., Ozaki, T., Park, J., Sakawa, Y., Takabe, H., Williams, G. & Zhang, Z. (2013). New insights into the laser produced electron–positron pairs. *New J. Phys.* **15**, 065010.

Cowan, T.E., Roth, M., Johnson, J., Brown, C., Christl, M., Fountain, W., Hatchett, S., Henry, E.A., Hunt, A.W., Key, M.H., MacKinnon, A., Parnell, T., Pennington, D.M., Perry, M.D., Phillips, T.W., Sangster, T.C., Singh, M., Snavely, R., Stoyer, M., Takahashi, Y., Wilks, S.C. & Yasuike, K. (2000). Intense electron and proton beams from PetaWatt laser–matter interactions. *Nucl. Instrum. Methods Phys. Res. A* **455**, 13.

Geng, J.J., Wu, X.F., Huang, Y.F., Li, L. & Dai, Z.G. (2016). Imprints of electron–positron winds on the multi wave-length afterglows of gamma-ray bursts. *Astrophys. J.* **825**, 107.

Goldreich, P. & Julian, W.H. (1969). Pulsar electrodynamics. *Astrophys. J.* **157**, 869.

Haas, F., Manfredi, G. & Feix, M. (2000). Multistream model for quantum plasmas. *Phys. Rev. E* **62**, 2763.

Harris, M., Hill, C.A., Tapster, P.R. & Vaughan, J.M. (1994). Laser modes with helical wave fronts. *Phys. Rev. A* **49**, 3119.

Khan, S.A., Rehman, A.U. & Mendonca, J.T. (2014). Kinetic study of ion-acoustic plasma vortices. *Plasma Phys.* **21**, 092109.

Khan, Sh. A., Ali, S. & Mendonca, J.T. (2013). Plasmons carrying orbital angular momentum in quantum plasmas. *J. Plasma Phys.* **79**, 973–979.

Leach, J., Padgett, M.J., Barnett, S.M., Franke-Arnold, S. & Courtial, J. (2002). Measuring the orbital angular momentum of a single photon. *Phys. Rev. Lett.* **88**, 257901.

Leyser, T.B., Norin, L., Mc Carrick, M., Pedersen, T.R. & Gustavsson, B. (2009). Radio pumping of ionospheric plasma with orbital angular momentum. *Phys. Rev. Lett.* **102**, 065004.

Mehdian, H., Hajisharifi, K., Azadnia, F. & Tajik-Nezhad, S. (2016). Magnetorotational instability of weakly ionized and magnetized electron–positron-ion plasma. *Phys. Plasmas* **23**, 102903.

Mendonca, J.T. (2012). Kinetic description of electron plasma waves with orbital angular momentum. *Phys. Plasmas* **19**, 112113.

Mendonca, J.T., Ali, S. & Thide, B. (2009). Plasmons with orbital angular momentum. *Phys. Plasmas* **16**, 112103.

Michel, F.C. (1991). *Theory of Neutron Star Magnetosphere*. Chicago, IL: Chicago University Press.

Miller, H.R. & Witter, P.J. (1987). *Active Galactic Nuclei*. Berlin: Springer.

Misner, W., Thorne, K. & Wheeler, J.A. (1973). *Gravitation*. San Francisco, CA: Freeman.

Nekrasov, A.K. (2009). Compressible streaming instabilities in rotating thermal viscous objects. *Astrophys. J.* **704**, 80–88.

https://doi.org/10.1017/S0263034617000441 Published online by Cambridge University Press

Rees, M.J. (1983). *In The Very Early Universe*. Cambridge: Cambridge University Press.
Rehman, A.U., Ali, S., Khan, S.A., Shahzad, K. (2016). Twisted electron-acoustic waves in plasmas. *Plasma Phys*. **23**, 082122.
Saleem, H., Haque, Q. & Vranjes, J. (2003). Nonlinear drift waves in electron–positron–ion plasmas. *Phys. Rev. E* **67**, 057402.
Saleem, H. & Khan, R. (2005). Two-Stream instabilities in electron–positron–ion plasmas. *Phys. Scr*. **71**, 314–317.
Schlickeiser, R., Pohl, M. & Vainio, R. (2003). The influence of electron impact ionization in the relativistic pickup of interstellar neutrals. *Astrophys. J*. **596**, 840.
Shukla, P.K. (2013). Twisted electrostatic ion-cyclotron waves in dusty plasma. *Phys. Rev. E* **87**, 015101.
Shukla, P.K., Eliasson, B. & Stenflo, L. (2012). Stimulated scattering of electromagnetic waves carrying orbital angular momentum in quantum plasmas. *Phys. Rev. E* **86**, 016403.
Shukla, P.K., Mamun, A.A. & Stenflo, L. (2003). Vortices in a strongly magnetized electron–positron–ion plasma. *Phys. Scr*. **68**, 295–297.
Stockem Novo, A., Yoon, P.H., Lazar, M., Schlickeiser, R., Poedts, S. & Seough, J. (2015). Quasilinear saturation of the aperiodic ordinary mode streaming instability. *Phys. Plasmas* **22**, 092301.
Surko, C.M. & Murphy, T. (1990). Use of the positron as a plasma particle. *Phys. Fluids B* **2**, 1372.
Tandberg-Hansen, E. & Emshie, A.G. (1988). *The Physics of Solar Flares*. Cambridge: Cambridge University Press.
Tinakiche, N. & Annou, R. (2015). Oscillating two-stream instability in a magnetized electron–positron–ion plasma. *Phys. Plasmas* **22**, 042101.
Verdon, M.W. & Melrose, D.B. (2008). Wave dispersion in a counter-streaming, cold, magnetized, electron–positron plasma. *Phys. Rev. E* **77**, 046403.

APPENDIX A: L–G POTENTIAL AND ELECTRIC FIELD

For electrostatic twisted modes propagating along the $\hat{z}$-axis with slowly varying amplitude, the potential function can satisfy the paraxial equation as

$$\left(\nabla_{\perp}^{2} + 2ik_z\frac{\partial}{\partial z}\right)\phi(\boldsymbol{r}, t) = 0. \tag{A1}$$

Here $\nabla_{\perp}^{2} = (1/r)\partial/\partial r\left(r\partial/\partial r\right) + \left(1/r^2\right)\partial^2/\partial\varphi^2$ is the perpendicular component of Laplacian operator in the cylindrical coordinates. By solving Eq. (A1), one can obtain the LG potential for system which is described by superposition of LG functions as follows:

$$\phi(\boldsymbol{r}, t) = \sum_{jl}\tilde{\phi}_{jl}F_{jl}(r, z)\exp(il\theta + ik_z z - i\omega t) \tag{A2}$$

and

$$F_{jl}(r, z) = \frac{1}{2\sqrt{\pi}}\left\{(l+j)!/j!\right\}^{\frac{1}{2}}X^{|l|}L_j^{|l|}\exp\left(-\frac{X}{2}\right). \tag{A3}$$

where $\tilde{\phi}_{jl}$ is the mode amplitude, $j(= 0, 1, 2, \ldots)$ and $l(= 0, \pm 1, \pm 2, \ldots)$ are the radial and angular mode numbers, respectively. Also $X = r^2/w(z)^2$, $w(z)$ being the beam waist, θ is the azimuthal angle, and Laguerre polynomials are given as:

$$L_j^{|l|}(X) = \frac{\exp(X)}{Xj!}\frac{d^j}{dX^j}\left[X^{l+j}\exp(-X)\right]. \tag{A4}$$

Also, the LG modes satisfy the orthogonality conditions

$$F_{j'l'}|F_{jl} = \int_0^{2\pi}\int_0^{\infty} d\theta\, r\mathrm{d}r F_{j'l'}F_{jl}e^{i(l-l')\theta} = \delta_{jj'}\delta_{ll'}. \tag{A5}$$

Having the LG potential and using $\boldsymbol{E} = -\nabla\phi$, we can calculate the components of electric field in the cylindrical coordinates. The electric field components given by

$$E_r = -\frac{\phi(\boldsymbol{r}, t)}{F_{jl}}\frac{\partial F_{jl}}{\partial r}, \tag{A6}$$

$$E_\theta = -i\frac{l\phi(\boldsymbol{r}, t)}{r}, \tag{A7}$$

$$E_z = -\left(ik_z + \frac{1}{F_{jl}}\frac{\partial F_{jl}}{\partial z}\right)\phi(\boldsymbol{r}, t). \tag{A8}$$

This equations show that the electric field lines are not straight lines along the z-direction as in ordinary plane wave solutions, but are showing helical structures. With consider the $\boldsymbol{k}_{\mathrm{ef}} = \left\{(-i/F_{jl})\left(\partial F_{jl}/\partial r\right)\right\}\hat{e}_r + \left\{l/r\right\}\hat{e}_\theta + \left\{k_z - (i/F_{jl})\left(\partial F_{jl}/\partial z\right)\right\}\hat{e}_z$, the electric field can be represented as $\boldsymbol{E} = -i\boldsymbol{k}_{\mathrm{ef}}\phi(r, \varphi, z)$.

https://doi.org/10.1017/S0263034617000441 Published online by Cambridge University Press